Investigating the allosteric response of the PICK1 PDZ domain to

different ligands with all-atom simulations

Amy O. Stevens¹, I. Can Kazan², Banu Ozkan*², and Yi He*¹

¹Department of Chemistry & Chemical Biology, The University of New Mexico, Albuquerque, New Mexico

²Department of Physics, Center for Biological Physics, Arizona State University, Tempe, Arizona

Abstract

The PDZ family is comprised of small modular domains that play critical roles in the allosteric modulation of many cellular signaling processes by binding to the C-terminal tail of different proteins. As dominant modular proteins that interact with a diverse set of peptides, it is of particular interest to explore how different binding partners induce different allosteric effects on the same PDZ domain. Because the PICK1 PDZ domain can bind different types of ligands, it is an ideal test case to answer this question and explore the network of interactions that give rise to dynamic allostery. Here, we use all-atom molecular dynamics simulations to explore dynamic allostery in the PICK1 PDZ domain by modeling two PICK1 PDZ systems: PICK1 PDZ-DAT and PICK1 PDZ-GluR2. Our results suggest that ligand binding to the PICK1 PDZ domain induces dynamic allostery at the aA helix that is similar to what has been observed in other PDZ domains. We found that the PICK1 PDZ-ligand distance is directly correlated with both dynamic changes of the αA helix and the distance between the αA helix and βB strand. Furthermore, our work identifies a hydrophobic core between DAT/GluR2 and I35 as a key interaction in inducing such dynamic allostery. Finally, the unique interaction patterns between different binding partners and the PICK1 PDZ domain can induce unique dynamic changes to the PICK1 PDZ domain. We suspect that unique allosteric coupling patterns with different ligands may play a critical role in how PICK1 performs its biological functions in various signaling networks.

Introduction

PDZ (PSD-95/Dlg1/ZO-1) domains are highly abundant protein-protein interaction domains involved in regulating signaling pathways. They play a critical role in many biological processes, such as managing cell polarity, regulating tissue growth and development, trafficking of membrane protein receptors and ion channels, and regulating cellular pathways. PDZ domains have been identified in 151 unique human proteins. Despite the broad function and relatively low sequence identity within PDZ domains, the secondary structure is highly conserved. The canonical PDZ domains contain six β -strands and two α -helices and have a single binding site in the hydrophobic groove between the α B helix and the β B strand, as shown in Figure 1A. PDZ domains most commonly interact with the final three to five C-terminal residues of target proteins

via the carboxylate binding loop that is defined by the conserved χ - φ -Gly- φ motif, where χ is any residue and φ is any hydrophobic residue. Various groups have revealed how these highly conserved protein-protein interactions propagate allosteric effects through the PDZ domain. 13,14,23–27,15–22

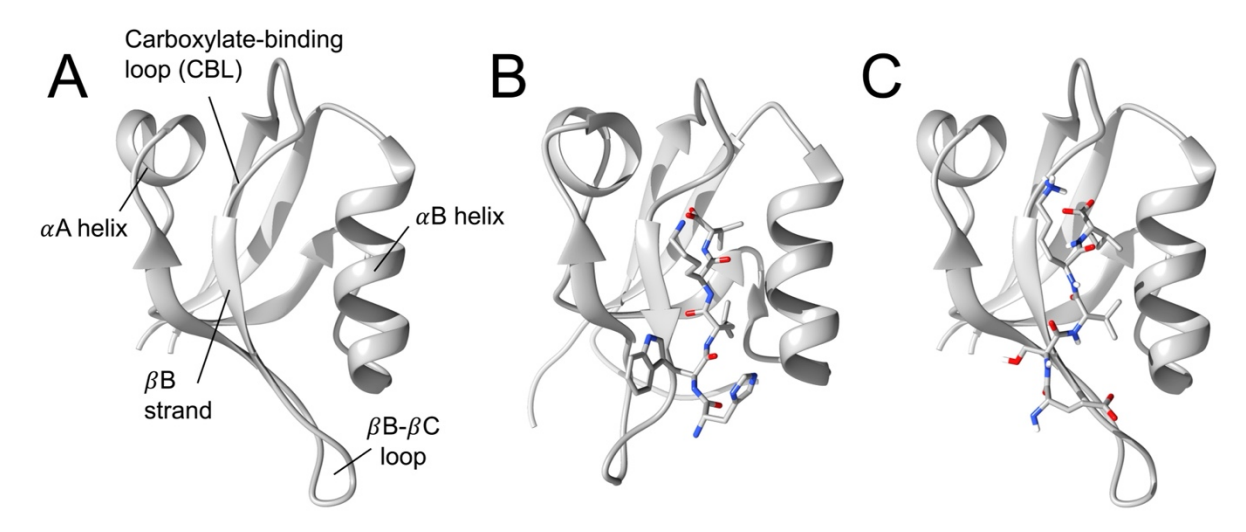


Figure 1. The PICK1 PDZ domain. (A) PICK1 PDZ domain with labeled secondary structures (PDB ID: 2PKU, ligand removed). (B) PICK1 PDZ-DAT complex (PDB ID: 2LUI). DAT ligand is the final five C-terminal residues of DAT (HWLKV). (C) PICK1 PDZ-GluR2 complex (PDB ID: 2PKU). GluR2 ligand is the final five C-terminal residues of AMPAR GluR2 (ESVKI). Notably, B-C are the starting structures of the all-atom MD simulations.

The PDZ domain is considered to be a model system to study allostery within small modular domains. Allostery in the PDZ family was initially brought to the table when Lockless and Ranganathan¹³ proposed a method to statistically predict allosteric residue networks using multiple sequence alignment. This method is based on networks of energetically coupled residues that are responsible for the propagation of allostery throughout the PDZ domain. This original work sparked a wide interest in studying allostery within the PDZ family. Many efforts have followed Lockless and Ranganathan's footsteps by applying various computational techniques, including direct coupling analysis, ^{28,29} deep coupling scan, ³⁰ anisotropic thermal diffusion, ^{31,32} rigid-residue scan,³³ and interaction correlation via molecular dynamics simulations,^{21,22,34} to reveal allosteric networks within the PDZ family. Furthermore, experimental groups have expanded our understanding of allostery in the PDZ family with applications of nuclear magnetic resonance (NMR)^{16,35,36} and mutational analyses.^{28,29,37} Despite the abundance of domains in the PDZ family, these efforts have primary focused on a few well-studied PDZ domains, including Par-6 PDZ, 38-⁴⁰ PSD-95 PDZ3, ^{17,20,23,36,37,41–45} PTP-1E PDZ2, ^{16,20,21,35,41,46} PTP-BL PDZ. ^{17,47} To the best of our knowledge, little attention has yet been given to explore allostery of the PDZ domain in Protein Interacting with C Kinase-1 (PICK1).

PICK1 is a scaffolding protein involved in regulating the trafficking of various membrane proteins via endocytosis. 48–50 PICK1 is an especially unique PDZ protein as it is the only protein in the

human proteome that is comprised of both a PDZ domain and a BAR (Bin/amphiphysin/Rvs) domain.^{51–53} The PICK1 PDZ domain forms protein-protein interactions with a variety of integral membrane proteins, including the Dopamine Transporter (DAT)⁵⁴ and the GluR2 subunit of the AMPA receptor.⁴⁸ Widely accepted hypotheses suspect that such PDZ-protein interactions lead to a propagation of signals through PICK1 that alters its interdomain dynamics.^{49,50} This global transduction of signal through PICK1 could be explained by allostery at the PICK1 PDZ domain. The presence of allostery at the PICK1 PDZ domain would have major implications in our understanding of the biological function of PICK1.

The purpose of this study is to use all-atom molecular dynamics (MD) simulations to reveal how the atomic-level interaction pattern affects the interaction mechanisms and dynamics between the PICK1 PDZ domain and two representative ligands. These ligands include the final five C-terminal residues of two natural ligands: DAT and AMPAR GluR2. The two systems of interest are shown in Figure 1B-C. Here, we see that both ligands induce dynamic allostery at the α A helix of the PICK1 PDZ domain. Furthermore, our results suggest that different ligands may trigger different dynamic changes to the PICK1 PDZ domain. Lastly, our work identifies that the hydrophobic core that is formed between the ligands and residue I35 may be key to inducing such dynamic allostery.

Methods

We studied two PICK1 PDZ systems: PICK1 PDZ-DAT complex and PICK1 PDZ-GluR2 complex. The DAT ligand refers to the final five C-terminal residues (HWLKV) of the Dopamine Transporter (DAT), and the GluR2 ligand refers to the final five C-terminal residues (ESVKI) of the carboxyl tail peptide of the AMPA receptor GluR2 subunit. Experimentally determined crystal structures of the complex systems were used to generate the starting structure for all all-atom molecular dynamics simulations. (PDB ID: 2LUI⁵⁵ and 2PKU,⁵⁶ respectively). The PDB file of the PICK1 PDZ-DAT complex (PDB ID: 2LUI) was manually edited by trimming terminal residues to ensure an identical sequence to the PICK1 PDZ-GluR2 system. Each starting structure is shown in Figure 1B-C. Each system was prepared using CHARMM-GUI. 57,58 The most recently developed CHARMM36m⁵⁹ force field with explicit solvent (TIP3P) was used in each simulation with the Groningen Machine for Chemical Simulations (GROMACS) package, 60-62 version 2020.4. Counter ions (Na⁺ or Cl⁻) were added to neutralize the systems at 293 K. Steepest-descent minimization and 1-ns MD equilibrium simulations were carried out to generate equilibrated starting structures for the MD simulations. All bonds with hydrogen atoms were converted to constraints with the algorithm LINear Constraint Solver (LINCS) ⁶³. A Nose-Hoover temperature thermostat^{64,65} was used in each simulation. The time step was set as 2 fs, and snapshots were taken every 100 ps. Each system was built in a 90 Å × 90 Å cubic water box. Each system (PICK1 PDZ-DAT and PICK1 PDZ-GluR2) had four replicates at 7 µs per trajectory, a total of 28 µs (4 × 7µs) per system.

Defining the bound state

The PICK1 PDZ-DAT and PICK1 PDZ-GluR2 complex systems had various dissociation events over the four trajectories (Figure S1). It is important to define a boundary that separates the bound states from the unbound states. Because the PICK1 PDZ-ligand complexes were very dynamic, we considered the distance distributions (Figure S2 and S3) of four key binding residue pairs that have been previously identified^{55,56} between the PICK1 PDZ domain and the ligands. For the PICK1 PDZ-DAT and PICK1 PDZ-GluR2 complexes, residue pairs I37-L-2 and I37-V-2, respectively, display the clearest distinction on average between the bound state and unbound states. With these state-defining residue pairs, frames were classified bound or unbound. A bound state is defined as a distance less than 5.0 Å between any two atoms in I37 and L-2 for the PICK1 PDZ-DAT complex, and a distance less than 5.0 Å between any two atoms on I37-V₋₂ for the PICK1 PDZ-GluR2 complex. To test the accuracy of the defined cutoff, cluster analysis was performed over the bound state trajectories to reveal the most probable positions of DAT and GluR2 about the PIKC1 PDZ domain. In this way, we obtained the five most probable clusters of each ligand. Figure 2 shows the PICK1 PDZ domain in gray while the most probable positions of the DAT (A) and GluR2 (B) are shown by unique colors. Our results confirm that the ligands reside in the PICK1 PDZ binding pocket in the defined bound state trajectories.

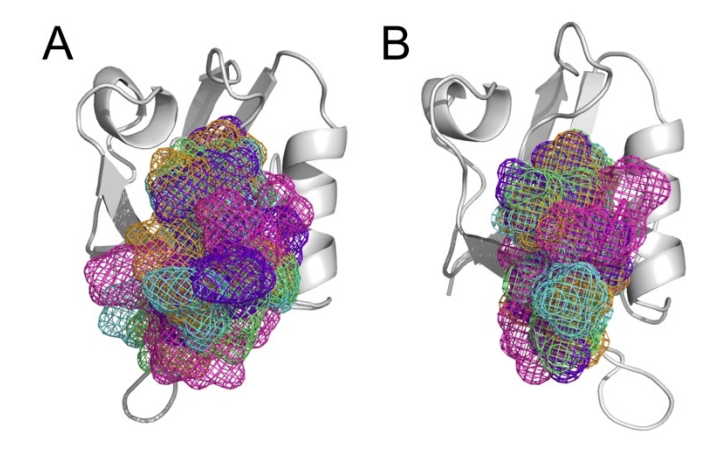


Figure 2. Cluster analysis reveals the most probable states of the (A) DAT and (B) GluR2 about the PICK1 PDZ domain after dividing the trajectories into bound states. The PICK1 PDZ domain is shown in gray and each cluster of the ligands is shown in a unique color. (A) Cluster 1 (orange) represents 62.7% of the frames, Cluster 2 (purple) represents 20.4% of the frames, Cluster 3 (pink) represents 8.1% of the frames, and Cluster 4 (green) represents 7.8% of the frames. Cluster 5 was excluded because if represents less than 1% of the frames. (B) Cluster 1 (orange) represents 37.1% of the frames, Cluster 2 (purple) represents 22.0% of the frames, Cluster 3 (pink) represents 20.8% of the frames, Cluster 4 (green) represents 10.8% of the frames, and Cluster 5 (blue) represents 9.3% of the frames.

Dynamic Flexibility Index (DFI)

The DFI metric estimates the resilience of residues within a given protein system. Being a residue specific metric, DFI calculates relative flexibility scores.⁶⁶ By incorporating Linear Response Theory (LRT) and Perturbation Response Scanning (PRS),⁶⁷ DFI calculates the response of a residue due to a perturbation on another residue normalized by the average response of all residues in the protein.⁴¹ Position specific dynamics profiles are calculated by utilizing residue covariances.

$$[\Delta \mathbf{R}]_{3N\times 1} = [\mathbf{H}]_{3N\times 3N}^{-1} [\mathbf{F}]_{3N\times 1}$$

$$DFI_i = \frac{\sum_{j=1}^{N} \left| \Delta R^j \right|_i}{\sum_{i=1}^{N} \sum_{j=1}^{N} \left| \Delta R^j \right|_i}$$

The Hessian matrix, H, contains the second derivative of potentials. Residue covariances are calculated by taking the inverse of the Hessian matrix, H^{-1} . The Elastic Network Model (ENM) is commonly used to produce the Hessian matrix. However, to include explicit solvent and better estimate residue interactions, residue covariances can be gathered from an MD simulation production trajectory. In this study, we utilized the MD simulations to calculate residue covariances. ΔR is a response vector calculated by multiplying the covariance matrix with the force vector, F and contains the residue responses. The collection of DFI values calculated from this approach is further refined with a percentile ranking to normalize the scores. A residue with a DFI score less than 0.2 is considered a rigid location, while a position with a DFI score higher than 0.8 is considered a flexible residue. Rigid residues have been found to be important in protein stability and function. 68

Dynamic Coupling Index (DCI)

Utilizing the same elemental principles as described above, the DCI metric captures the dynamic allosteric coupling of pair of residues in a protein. DCI calculates the response of a residue due to a Brownian force applied to another residue in the same system normalized by the average response of the same residue due to perturbations on the rest of the proteins. The magnitude of the response represents the strength of the dynamic allosteric coupling of a site to another residue being perturbed.

$$DCI_{i} = \frac{\sum_{j}^{N_{Functional}} \left| \Delta R^{j} \right|_{i} / N_{Functional}}{\sum_{j=1}^{N} \left| \Delta R^{j} \right|_{i} / N}$$

A DCI score applied on binding site residues can reveal other residues in the protein that are highly coupled, meaning a binding event or the dynamics of the residue upon binding will be highly affected. Notably, the DCI score is not an indicator of binding dynamics but rather how the binding dynamics are coupled to the rest of the protein. DCI metric can uncover long range allosteric communications related to the binding event. ^{66,69,70} Residues with a high DCI score indicate strong

coupling with binding site and a position with a low DCI score is considered weakly coupled to the binding site.

Network Analysis

Network analysis calculates the correlated movements between residues within a protein or protein complex by constructing residue-based and community-based weighted network graphs according to a trajectory. During the calculations, each residue is represented by a node in a network and the links between nodes are the cross-correlation values between these nodes. By using the algorithm developed by McCammon, A. J. and Harvey, S. C.,⁷¹ the displacement of the Ca atoms are used to assess the magnitude of all pairwise cross-correlation coefficients. If the correlation value is 1, the fluctuations of two Ca atoms are completely correlated. If the correlation value is -1, the fluctuations of two Ca atoms are completely anticorrelated (same period and opposite phase). Lastly, if the correlation value is 0, the fluctuations of two Ca atoms are not correlated. The analysis uses the calculated cross-correlation coefficients to return a community partition with the highest overall modularity value based on Girvan-Newman style clustering.⁷² All the above analysis was carried out using the bio3d package^{73–75}.

Local Frustration Evaluations

To quantify the degree of local frustration associated with the binding of different ligands to the PICK1 PDZ domain, the Frustratometer server (http://frustratometer.qb.fcen.uba.ar/)</br>
76-78 was used to evaluate the two PDZ-ligand complexes investigated here. Default parameters were used when carrying out the assessments of local frustration, e.g., a 5Å radius cutoff value was applied. The PDB structures used in local frustration analysis contained only the PDZ domain, and the ligands have been removed.

Results

Each trajectory experienced ligand dissociation events (Figure S1). These dissociation events present a unique opportunity to explore the switching of dynamic states at the αA helix in real-time. First, we reveal the unique and specific ligand-protein interactions related to the dissociation events by performing hydrogen bond analysis across the two complex systems. Hydrogen bond analysis reveals canonical Class II PDZ-ligand interactions with the carboxylate-binding loop in each system (Figure 3). These results are in good agreement with previous experimental work. Additionally, we performed a statistical analysis to rank the probability of each hydrogen bond forming in the binding pocket (Figure S4-5). The PICK1 PDZ-DAT system has three hydrogen bonds that occur in at least 90% of the bound frames, including I37(N)-L-2(O), L-2(N)-I37(O) and V₀(N)-I35(O) (Figure S4). The PICK1 PDZ-GluR2 system has three hydrogen bonds that occur in at least 70% of frames with the ligand bound, including I₀(N)-I35(O), I37(N)-V-2(O) and V-2(N)-I37(O) (Figure S5). These three most probable pairs in each system are in agreement with each other. In both systems, the most probable hydrogen bonds occur between (1) I37 and the residue

at position P_{-2} of the ligand and (2) I35 and the residue at position P_0 of the ligand. These interactions are much more prevalent than interactions between G34- P_0 and I33- P_0 .

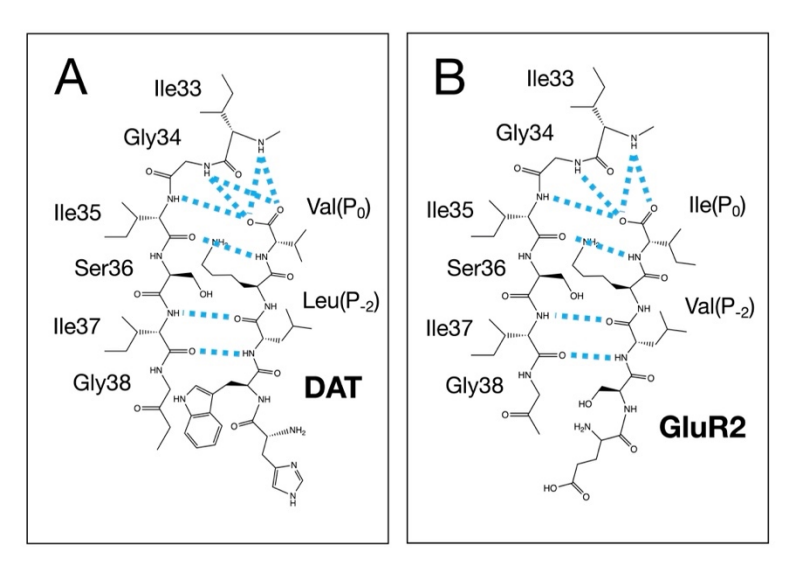


Figure 3. Hydrogen bonding network at the binding pocket of the (A) PICK1 PDZ-DAT complex and (B) PICK1 PDZ-GluR2 complex. PDZ-DAT and PDZ-GluR2 display a similar pattern of hydrogen bonding.

While the above analysis reveals the most probable hydrogen bonds within each complex, it is unclear if these interactions are simply essential to the stability of complex formation or, ultimately, if they effect the overall dynamics and subsequent dynamic allostery of the system. To connect the changes in protein-ligand hydrogen bonding interactions (particularly, as related to ligand dissociation) to protein dynamics, we explored the correlation between ligand dissociation and the dynamics of PICK1 PDZ domain by calculating the coupling of various residue-residue distance pairs over the first 3 ms of each trajectory. Five pairs were considered in the coupling calculation: I33-P₀, G34-P₋₁, I35-P₋₂, S36-P₋₃ and I37-P₋₄. The five PICK1 PDZ residues were chosen because they comprise the βB strand which has been identified as a key player in ligand binding by previous work. 11 These pairs were selected to represent the overall interactions between PICK1 PDZ domain and ligand. Figure S6 lists the twenty residue-residue pairs for each system that are most strongly correlated with the distance changes between the five selected pairs. Having the relative highest rank in both systems, we consider the distance between I33 (βB strand) and A58 (αA helix) as directly dependent on the atomic-level interactions between the PICK1 PDZ domain and ligand. Interestingly, the I33-A58 distance can also be used to describe the overall distance between the β B strand and the α A helix. We explore the correlation between the PDZ-ligand interactions and the distance between the βB strand and the αA helix below.

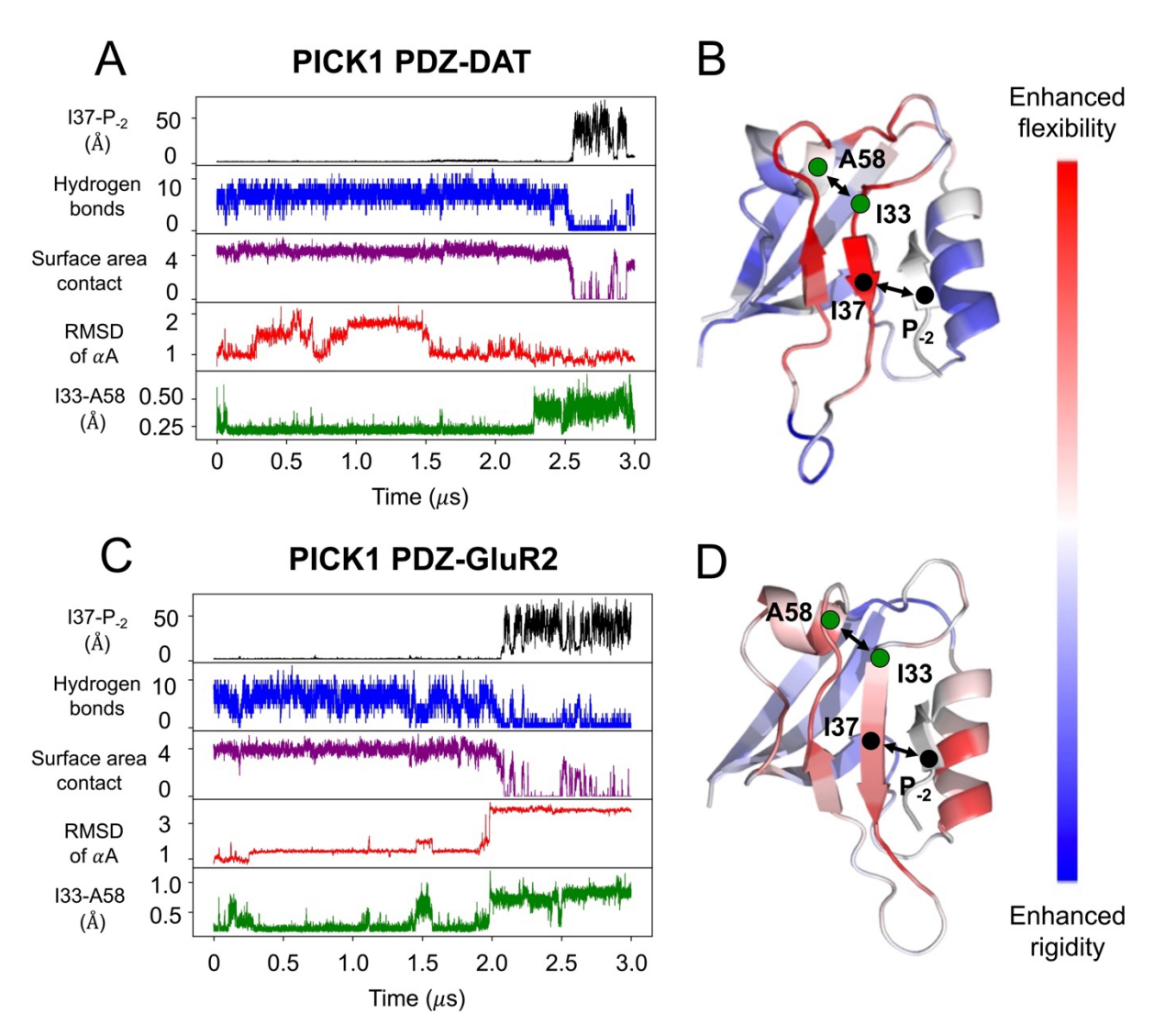


Figure 4. Correlation between ligand dissociation and the dynamics of the PICK1 PDZ domain. (A) Representative PDZ-DAT trajectory. At ~2.5 μ s, the distance between 137 of PICK1 PDZ and L-2 of DAT increases (black, A.A), the number of hydrogen bonds between the PICK1 PDZ domain and DAT decreases (blue), the surface area contact between the PICK1 PDZ domain and DAT decreases (purple), the RMSD of the αA helix does not appear to correlate with ligand dissociation (red), and the residue-residue distance between 133 of the βB stand and A58 of the αA helix increases (green). (B) ΔDFI between the bound and unbound states of the PICK1 PDZ-DAT trajectory 1. ΔDFI of PDZ-DAT indicates little change in the flexibility of the αA helix upon ligand dissociation. (C) Representative PDZ-GluR2 trajectory. At ~2 μ s, the distance between 137 of PICK1 PDZ and V-2 of GluR2 increases (black), the number of hydrogen bonds between the PICK1 PDZ domain and GluR2 decreases (blue), the surface area contact between the PICK1 PDZ domain and GluR2 decreases (purple), the RMSD of the αA helix increases (red), and the residue-residue distance between 133 of the βB-stand and A58 of the αA helix increases (green). (D) ΔDFI between the bound and unbound states of the PICK1 PDZ-GluR2 trajectory 4. ΔDFI shows an enhanced flexibility of the αA helix upon GluR2 dissociation.

Figure 4 describes representative dissociation events for the PICK1 PDZ-DAT (Figure 4A-B) and PICK1 PDZ-GluR2 systems (Figure 4C-D). First, we will consider PICK1 PDZ-DAT system, where the dissociation of the DAT is weakly correlated with the dynamics of the aA helix (Figure 4A-B). The distance between I37 of the PICK1 PDZ domain and L-2 of DAT was used to trace the dissociation as defined in the Methods section. At ~2.5 ms, the distance between I37 and L-2 spikes as the ligand dissociates from the binding pocket (Figure 4A, black). This dissociation is confirmed by hydrogen bond and surface area analysis. As DAT dissociates, the number of hydrogen bonds and the surface area between the PICK1 PDZ domain and DAT drops to zero (Figure 4A, blue and purple, respectively). The surface area between the PICK1 PDZ domain and DAT was calculated using solvent-accessible surface area. While the dissociation event does not clearly correlate with the RMSD of the αA helix (Figure 4A, red), it does result in a distinct increase in distance between αA helix and the βB strand (Figure 4A, green).

Next, we will consider the representative dissociation event for the PICK1 PDZ-GluR2 system (Figure 4C-D). As shown in Figure 4C, the dissociation of the GluR2 is directly correlated with the dynamics of the αA helix. The dissociation of GluR2 at ~2.0 μs is confirmed by a sharp distance increase between I37 of the PICK1 PDZ domain and V-2 of GluR2 (Figure 4C, black), a loss of hydrogen bonds between the PICK1 PDZ domain and GluR2 (Figure 4C, blue), and a loss of surface area contact between the PICK1 PDZ domain and GluR2 (Figure 4C, purple). Interestingly, the disruption of PICK1 PDZ-GluR2 interactions is correlated with dynamic changes at the αA helix. Figure 4C (red) shows that the RMSD of the αA helix increases with the dissociation of GluR2. Moreover, our analysis reveals a correlation between PICK1 PDZ-GluR2 interactions and the distance between the βB strand and the αA helix (Figure 4C, green). This distance separation may play a role in the destabilization of the αA helix.

Finally, we calculated the change in the dynamics flexibility index (ΔDFI) across the bound and unbound states of each system (Figure 4B and 4D). ΔDFI reveals significant changes in dynamics of the PICK1 PDZ domain due to the dissociation of ligands. The important ligand binding regions, including the αB helix and βB strand, show enhanced flexibility upon ligand dissociation. When the interactions are disrupted, the key binding residues gain more conformational freedom, and the flexibility enhances. Thus, enhanced flexibility at the binding site is a direct indicator of a dissociation. More interestingly, ΔDFI also reveals unique changes to the αA helix upon dissociation of each unique ligand. As represented by the RMSD of the αA helix (Figure 4A, red), the dissociation of DAT does not enhance the flexibility of the αA helix (Figure 4B). Instead, the majority of the αA helix has little change in terms of flexibility while A59 shows enhanced rigidity (Figure 4B). Oppositely, there are significant changes in dynamics of the αA helix due to the dissociation of GluR2 (Figure 4D). Echoing the RMSD of the αA helix (Figure 4C, red) and the distance between I33 and A58 (Figure 4C, green), DFI analysis shows enhanced flexibility at the αA helix upon ligand dissociation (Figure 4D). As the I33-A58 distance increases, the interactions

between the αA helix and the carboxylate-binding loop become weaker to allow more fluctuations. Advancing to a dynamically more flexible regime, the αA helix is observed be to allosterically being altered by the dissociation event.

To further explore the correlation between ligand binding and the dynamics at the αA helix, we performed protein network analysis. Protein network analysis can reveal the coupling of major movements by creating protein structure networks based on the primary motions of each residue. The analysis reveals the residues within the PICK1 PDZ domain that are most strongly coupled to the ligands' motion. The motions of DAT (Figure 5A) and GluR2 (Figure 5B) are both coupled to the motion of the distal αA helix and the βB - βC loop of the PICK1 PDZ domain. Interestingly, the motions of DAT are more strongly coupled to the βB and βC strands than are the motions of GluR2.

Dynamic Coupling Index (DCI) was applied to each system to explore the coupling of dynamics between binding site residues and the global protein. The DCI metric has previously been shown to capture allosteric coupling of distal site to critically important residues in a protein. Upon a binding event, the binding site residues experience exerted forces from the ligand so that the dynamics of the system may be affected. Notably, the force exerted by the ligand not only affects the dynamics of the binding site residues but may also affect the dynamics of the global protein due to allosteric communication. The DCI metric measures the coupling strength of a residue to a binding site. A highly coupled residue will experience the repercussions of binding more than weakly coupled residues. As shown in Figure 5C-D, DCI analysis on the PICK1 PDZ-DAT and PICK1 PDZ-GluR2 systems reveals a coupling trend that echoes results from network analysis at the α A helix. Both DAT and GluR2 binding residues observes strong coupling to the α A helix.

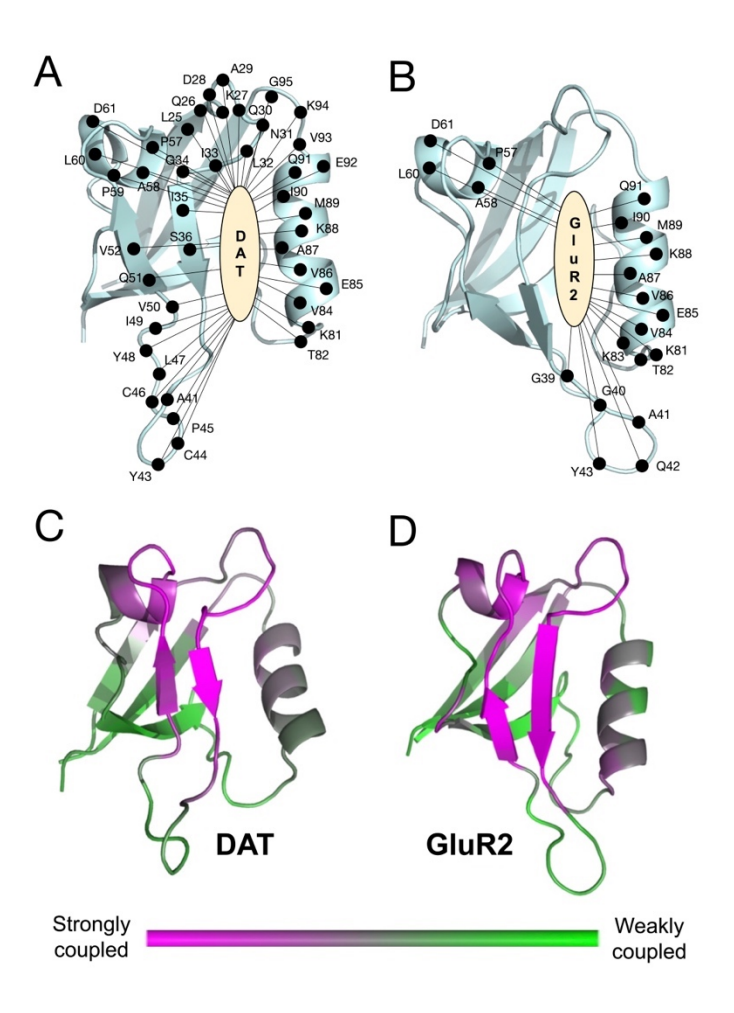
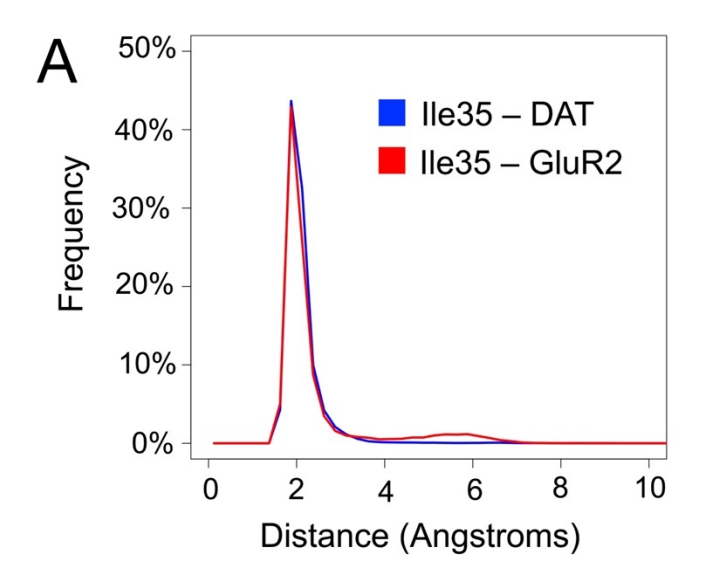


Figure 5. Allosteric dynamic coupling within the PICK1 PDZ-ligand systems. (A) Protein structure network analysis of the PICK1 PDZ-DAT system. (B) Protein structure network analysis of the PICK1 PDZ-GluR2 system. The motions of DAT and GluR2 are both coupled with the distal αA helix. (C) DCI analysis of the PICK1 PDZ-DAT system. (D) DCI analysis of the PICK1 PDZ-GluR2 system. In both systems, the binding residues of the PICK1 PDZ domain are coupled with the αA helix.

Time-resolved force distribution analysis (TRFDA)⁸⁰ was performed to reveal the punctual stress on each PICK1 PDZ residue as a result of ligand binding. TRFDA was performed over each trajectory, and the per trajectory results were summed over each complex system. The summed results are shown in Figure S7. The ten PICK1 PDZ residues that experienced the greatest punctual stress for each system are listed in Figure S8. Both DAT and GluR2 induce the greatest punctual stress on the β B strand and α B helix, regions that directly interact with the ligands. In the PICK1 PDZ-DAT system, all six residues that experience the greatest punctual stress comprise the β B strand. Oppositely, GluR2 induces significant punctual stress on K83 of the α B helix. These results point to the different interaction patterns induced by different ligands binding.

Our analysis reveals that DAT and GluR2 can induce unique stresses on the PICK1 PDZ domain, but the specific residues and mechanisms through which dynamic allostery is propagated in the PICK1 PDZ domain remains in question. A recent review of allostery in the PDZ family⁸¹ notes that A46 (\alpha A helix) of PTP-BL PDZ2 and A347 (\alpha A helix) of PSD-95 PDZ3 have been consistently identified as allosteric residues in a wide array of computational and experimental efforts. 15,18,85,31,34,35,41,46,82-84 Furthermore, in a recent work exploring the interactions and dynamics between the PICK1 PDZ domain and the small molecule inhibitor BIO124, we propose that a structural alignment of PICK1 PDZ, PTP-BL PDZ2, and PSD-95 PDZ3 suggests that this allosteric alanine residue on the αA helix is evolutionarily conserved across all three PDZ domains. 86 This structural alignment also suggests that the interactions between BIO124 and I35 of the PICK1 PDZ domain may have a role in the propagation of signal to A58 of the αA helix.⁸⁶ Notably, A58 forms a van der Waals surface with I35, which is directly involved in ligand binding. Here, our results support the importance of A58 as an allosteric residue in the PICK1 PDZ domain. Distance analysis reveals that I33-A58 distance is coupled with ligand binding, protein network analysis identifies A58 in the network of residues dynamically coupled to the ligand, and DCI analysis indicates A58 is strongly coupled to binding site residues. We suspect that interactions between natural ligands and I35 of the PICK1 PDZ domain may also have a role in the propagation of signal to the αA helix.

We explore the role of I35 in propagating allosteric signal to the αA helix of the PICK1 PDZ domain. Distance distribution and time-resolved force distribution analysis (TRFDA) are used to identify the degree of interactions between the ligands and I35. As shown in Figure 6A, distance distribution analysis was performed between the ligand and I35 for each system. Here, the distance is defined as the shortest distance between any two atoms in the ligand and I35. DAT (blue) and GluR2 (red) both form the close contact (\sim 2 Å) with I35. In addition to exploring the distance distribution between ligands and I35, we also calculated the punctual stress on I35 induced by the ligand by using TRFDA. As shown in Figure S8, I35 is one of the top five residues that experiences the greatest punctual stress in each system. Figure 6B lists the punctual stress on I35 induced by DAT and GluR2. GluR2 induces a slightly greater punctual stress on I35 than DAT does. As demonstrated by Figure 4, GluR2 is more strongly coupled to the αA helix than DAT is. This stronger coupling between GluR2 and the αA helix may be a result of the strong punctual stress at I35. Together, distance distribution analysis and TRFDA point to the importance of interactions between the ligand and I35 in inducing dynamic allostery at the αA helix of the PICK1 PDZ domain.



Punctual Stress (kJ/mol/nm)

	Ligand → Ile35
DAT	295.03
GluR2	312.28

Figure 6. The role of I35 in propagating allosteric signal. (A) Distance distribution between I35 of the PICK1 PDZ domain and the ligands. (B) Punctual stress on I35 of the PICK1 PDZ domain induced by the ligands.

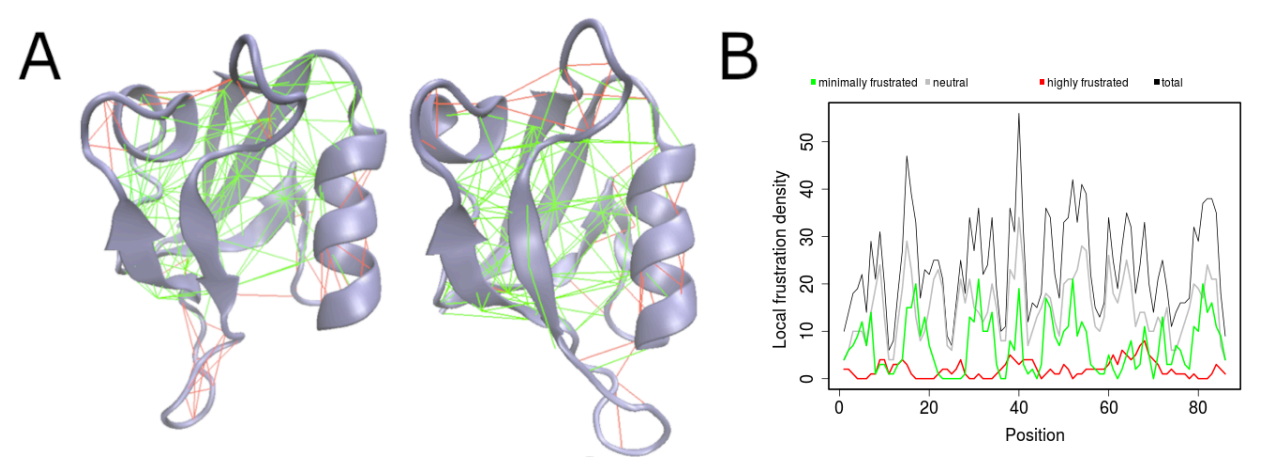


Figure 7. Local frustration in allosteric PICK1-PDZ domains. (A) The frustratograms for the individual conformations, with the minimally frustrated interactions in green lines, and the highly frustrated interactions in red lines. Left: PDB ID 2LUI, right: PDB ID 2PKU (B) Quantification of the local frustration projected on each residue of the PICK1-PDZ domain with minimally frustrated interactions (green) or highly frustrated interactions (red).

As discussed in previous work, the dynamic allostery can be closely related to the local conformational changes resulting from local frustrations. To explore the local frustration regions in PICK1 PDZ domains, the Frustratometer server was used. It can be seen from Fig. 7A that the αA helix is indeed a local high frustration region. Moreover, there are other local frustration regions, e.g., αB and βB - βC loop, which contain highly frustrated interactions. Interestingly, both of these two regions were identified in our network analysis (Fig. 5), showing their correlations with the ligands. The tight green lines at the center highlight that the major structural 'core' is conserved. The frustration projection on each residue is shown in Fig. 7B. The ligands are part of the core and, at the same time, trigger frustration on the protein surface.

Discussion

The purpose of this work is to investigate the dynamic allostery in the PICK1 PDZ domain that can be induced by unique binding partners. We found that (1) the PICK1 PDZ domain exhibits dynamic allostery at the αA helix, (2) the unique interaction patterns between different binding partners and the PICK1 PDZ may induce unique dynamic changes to the PICK1 PDZ domain, and (3) the hydrophobic core that is formed between the ligands and I35 may be key to inducing dynamic allostery at the αA helix.

Our results demonstrate that natural ligands DAT and GluR2 can induce dynamic allostery at the αA helix of the PICK1 PDZ domain. Protein structure network, DCI, TRFDA, and local frustration analysis show that both DAT and GluR2 are dynamically correlated with the αA helix. This dynamic correlation distant from the binding pocket points to the ability of DAT and GluR2 to induce dynamic allostery across the PICK1 PDZ domain. These results are in agreement with previous work which has identified the αA helix as an allosteric region within other PDZ domains, including Par-6 PDZ, PTP-1E PDZ2, PTP-BL PDZ1, and AF-6 PDZ. $^{16,19-21,38,46,47}$ Furthermore, dissociation events captured during our simulations presented a unique opportunity to explore dynamic changes to the PICK1 PDZ domain in real time. GluR2 dissociation is directly coupled with increased fluctuations at the αA helix and increased distance between the αA helix and the βB strand. The distant shift of the αA helix and the βB strand agrees with secondary structure shifts seen in previously studied PDZ domains. 21,22 Notably, the dissociation of the PICK1 PDZ-DAT complex was not so clearly correlated to dynamic changes at the αA helix. These results suggest that different binding partners may induce different dynamic changes to the PICK1 PDZ domain.

Previous work on the PTP-BL PDZ2 domain 17,35 and the PSD-95 PDZ3 domain 13 has pointed to the importance of structural equivalents of I35 in propagating allosteric signal to the αA helix. Our work suggests that I35 may also be a key residue in propagating signals in the PICK1 PDZ domain. Our results demonstrate that both DAT and GluR2 are dynamically coupled with the αA helix. Distance distribution analysis and TRFDA reveal that DAT and GluR2 form the close contact with

and induce the strong punctual stress on I35. These results suggest that interactions between the ligand and I35 are key to inducing dynamic allostery at the αA helix in the PICK1 PDZ domain. The release of the AlphaFold 2 provides a high-resolution solution^{87,88} to compare PDZ domains across multiple species and different proteins,

Our results identify dynamic allostery within the PICK1 PDZ domain. By comparing the responses of the PICK1 PDZ domain to the binding of different ligands, we see that the binding of different types of ligands may induce different dynamic changes to PICK1 PDZ domain. Our previous work on the PICK1 protein identified the αA helix of the PDZ domain as a key participant in interdomain PDZ-BAR and PDZ-linker interactions. ⁸⁹ We suspect that the ligand-induced dynamic changes at the αA helix may affect interdomain interactions and ultimately explain the long hypothesized conformational change of PICK1 upon ligand binding. ^{49,50} An atomic-level resolution of the mechanism behind the PICK1 interdomain dynamics may greatly affect how we understand the PICK1 protein.

Supporting Information

Additional figures as mentioned in the text. All the simulation data can be shared upon email request.

Acknowledgement

This research was funded by the National Science Foundation Graduate Research Fellowship Program (Grant No. DGE-1939267), the National Science Foundation (Grant No. 2137558), the National Science Foundation (Grant No. 1901709), the Leverhulme Trust (RPG-2017-222), and the Gordon and Betty Moore Foundation (Award: 1715591). This work was also supported by the Substance Use Disorders Grand Challenge Pilot Research Award, the Research Allocations Committee (RAC) Award, and the University of New Mexico Office of the Vice President for Research WeR1 Faculty Success Program. We also acknowledge the Centre of Informatics - Tricity Academic Supercomputer & network (CI TASK) in Gdansk, Poland, for the availability of high-performance computing resources.

References

- 1. Kennedy MB (1995) Origin of PDZ (DHR, GLGF) domains. Trends Biochem. Sci. 20:350.
- 2. Ponting CP (1997) Evidence for PDZ domains in bacteria, yeast, and plants. Protein Sci. 6:464–468.
- 3. Morais Cabral JH, Petosa C, Sutcliffe MJ, Raza S, Byron O, Poy F, Marfatia SM, Chishti AH, Liddington RC (1996) Crystal structure of a PDZ domain. Nature 382:649–652.
- 4. Van Ham M, Hendriks W (2003) PDZ domains Glue and guide. Mol. Biol. Rep.
- 5. Kim E, Sheng M (2004) PDZ domain proteins of synapses. Nat. Rev. Neurosci.
- 6. Ye F, Zhang M (2013) Structures and target recognition modes of PDZ domains: Recurring themes and emerging pictures. Biochem. J.
- 7. Harris BZ, Lim WA (2001) Mechanisma and role of PDZ domains in signaling complex

- assembly. J. Cell Sci.
- 8. Brakeman PR, Lanahan AA, O'Brien R, Roche K, Barnes CA, Huganir RL, Worley PF (1997) Homer: A protein that selectively binds metabotropic glutamate receptors. Nature.
- 9. Romero G, Von Zastrow M, Friedman PA Role of PDZ Proteins in Regulating Trafficking, Signaling, and Function of GPCRs. Means, Motif, and Opportunity. In: Advances in Pharmacology.; 2011.
- 10. Luck K, Charbonnier S, Travé G (2012) The emerging contribution of sequence context to the specificity of protein interactions mediated by PDZ domains. FEBS Lett. 586:2648–2661.
- 11. Doyle DA, Lee A, Lewis J, Kim E, Sheng M, MacKinnon R (1996) Crystal structures of a complexed and peptide-free membrane protein-binding domain: Molecular basis of peptide recognition by PDZ. Cell.
- 12. Pedersen SW, Pedersen SB, Anker L, Hultqvist G, Kristensen AS, Jemth P, Strømgaard K (2014) Probing backbone hydrogen bonding in PDZ/ligand interactions by protein amide-to-ester mutations. Nat. Commun. 5:3215.
- 13. Lockless SW, Ranganathan R (1999) Evolutionarily conserved pathways of energetic connectivity in protein families. Science (80-.).
- 14. Tochio H, Hung F, Li M, Bredt DS, Zhang M (2000) Solution structure and backbone dynamics of the second PDZ domain of postsynaptic density-95. J. Mol. Biol.
- 15. Walma T, Spronk CAEM, Tessari M, Aelen J, Schepens J, Hendriks W, Vuister GW (2002) Structure, dynamics and binding characteristics of the second PDZ domain of PTP-BL. J. Mol. Biol. 316:1101–1110.
- 16. Fuentes EJ, Der CJ, Lee AL (2004) Ligand-dependent Dynamics and Intramolecular Signaling in a PDZ Domain. J. Mol. Biol. 335:1105–1115.
- 17. Gianni S, Walma T, Arcovito A, Calosci N, Bellelli A, Engström Å, Travaglini-Allocatelli C, Brunori M, Jemth P, Vuister GW (2006) Demonstration of Long-Range Interactions in a PDZ Domain by NMR, Kinetics, and Protein Engineering. Structure 14:1801–1809.
- 18. Dhulesia A, Gsponer J, Vendruscolo M (2008) Mapping of two networks of residues that exhibit structural and dynamical changes upon binding in a PDZ domain protein. J. Am. Chem. Soc. 130:8931–8939.
- 19. Niu X, Chen Q, Zhang J, Shen W, Shi Y, Wu J (2007) Interesting structural and dynamical behaviors exhibited by the AF-6 PDZ domain upon Bcr peptide binding. Biochemistry 46:15042–15053.
- 20. Morra G, Genoni A, Colombo G (2014) Mechanisms of differential allosteric modulation in homologous proteins: Insights from the analysis of internal dynamics and energetics of PDZ domains. J. Chem. Theory Comput. 10:5677–5689.
- 21. Lu C, Knecht V, Stock G (2016) Long-Range Conformational Response of a PDZ Domain to Ligand Binding and Release: A Molecular Dynamics Study. J. Chem. Theory Comput. 12:870–878.
- 22. Miño-Galaz GA (2015) Allosteric communication pathways and thermal rectification in pdz-2 protein: A computational study. J. Phys. Chem. B.
- 23. Kumawat A, Chakrabarty S (2017) Hidden electrostatic basis of dynamic allostery in a PDZ domain. Proc. Natl. Acad. Sci. U. S. A. 114:E5825–E5834.
- 24. De Los Rios P, Cecconi F, Pretre A, Dietler G, Michielin O, Piazza F, Juanico B (2005) Functional dynamics of PDZ binding domains: A normal-mode analysis. Biophys. J. 89:14–21.
- 25. Ossowski I von, Oksanen E, ... L von O-TF, 2006 undefined (2006) Crystal structure of the second PDZ domain of SAP97 in complex with a GluR-AC-terminal peptide. Wiley Online Libr.

- 273:5219-5229.
- 26. Grembecka J, Cierpicki T, Biochemistry YD-, 2006 undefined (2006) The Binding of the PDZ Tandem of Syntenin to Target Proteins,. ACS Publ. 45:3674–3683.
- 27. Chen Q, Niu X, Xu Y, Wu J, Shi Y (2007) Solution structure and backbone dynamics of the AF-6 PDZ domain/Bcr peptide complex. Protein Sci. 16:1053–1062.
- 28. Gianni S, Haq SR, Montemiglio LC, Jürgens MC, Engström Å, Chi CN, Brunori M, Jemth P (2011) Sequence-specific long range networks in PSD-95/Discs large/ZO-1 (PDZ) domains tune their binding selectivity. J. Biol. Chem. 286:27167–27175.
- 29. Hultqvist G, Haq SR, Punekar AS, Chi CN, Engström Å, Bach A, Strømgaard K, Selmer M, Gianni S, Jemth P (2013) Energetic pathway sampling in a protein interaction domain. Structure 21:1193–1202.
- 30. Olson CA, Wu NC, Sun R (2014) A comprehensive biophysical description of pairwise epistasis throughout an entire protein domain. Curr. Biol. 24:2643–2651.
- 31. Ota N, Agard DA (2005) Intramolecular signaling pathways revealed by modeling anisotropic thermal diffusion. J. Mol. Biol.
- 32. Ho BK, Agard DA (2010) Conserved tertiary couplings stabilize elements in the PDZ fold, leading to characteristic patterns of domain conformational flexibility. Protein Sci.
- 33. Kalescky R, Zhou H, Liu J, Tao P (2016) Rigid Residue Scan Simulations Systematically Reveal Residue Entropic Roles in Protein Allostery. PLoS Comput. Biol. 12:1004893.
- 34. Kong Y, Karplus M (2009) Signaling pathways of PDZ2 domain: A molecular dynamics interaction correlation analysis. Proteins Struct. Funct. Bioinforma. 74:145–154.
- 35. Fuentes EJ, Gilmore SA, Mauldin R V., Lee AL (2006) Evaluation of Energetic and Dynamic Coupling Networks in a PDZ Domain Protein. J. Mol. Biol.
- 36. Petit CM, Zhang J, Sapienza PJ, Fuentes EJ, Lee AL (2009) Hidden dynamic allostery in a PDZ domain. Proc. Natl. Acad. Sci. U. S. A.
- 37. Chi CN, Elfström L, Shi Y, Snäll T, Engström Å, Jemth P (2008) Reassessing a sparse energetic network within a single protein domain. Proc. Natl. Acad. Sci. U. S. A. 105:4679–4684.
- 38. Peterson FC, Penkert RR, Volkman BF, Prehoda KE (2004) Cdc42 regulates the Par-6 PDZ domain through an allosteric CRIB-PDZ transition. Mol. Cell 13:665–676.
- 39. Whitney DS, Peterson FC, Volkman BF (2011) A conformational switch in the CRIB-PDZ module of Par-6. Structure 19:1711–1722.
- 40. Thayer KM, Lakhani B, Beveridge DL (2017) Molecular Dynamics-Markov State Model of Protein Ligand Binding and Allostery in CRIB-PDZ: Conformational Selection and Induced Fit. J. Phys. Chem. B 121:5509–5514.
- 41. Gerek ZN, Ozkan SB (2011) Change in allosteric network affects binding affinities of PDZ domains: Analysis through perturbation response scanning. PLoS Comput. Biol.
- 42. Bozovic O, Jankovic B, Hamm P (2020) Sensing the allosteric force. Nat. Commun. 11:1–7.
- 43. Bozovic O, Zanobini C, Gulzar A, Jankovic B, Buhrke D, Post M, Wolf S, Stock G, Hamm P (2020) Real-time observation of ligand-induced allosteric transitions in a PDZ domain. Proc. Natl. Acad. Sci. U. S. A. 117:26031–26039.
- 44. Guclu TF, Kocatug N, Atilgan AR, Atilgan C (2021) N-Terminus of the Third PDZ Domain of PSD-95 Orchestrates Allosteric Communication for Selective Ligand Binding. J. Chem. Inf. Model. 61:347–357.
- 45. Kumawat A, Chakrabarty S (2020) Protonation-Induced Dynamic Allostery in PDZ Domain: Evidence of Perturbation-Independent Universal Response Network. J. Phys. Chem. Lett.:9026—

9031.

- 46. Cilia E, Vuister GW, Lenaerts T (2012) Accurate Prediction of the Dynamical Changes within the Second PDZ Domain of PTP1e. PLoS Comput. Biol.
- 47. Van Den Berk LCJ, Landi E, Walma T, Vuister GW, Dente L, Hendriks WJAJ (2007) An allosteric intramolecular PDZ-PDZ interaction modulates PTP-BL PDZ2 binding specificity. Biochemistry 46:13629–13637.
- 48. Dev KK, Nishimune A, Henley JM, Nakanishi S (1999) The protein kinase Cα binding protein PICK1 interacts with short but not long form alternative splice variants of AMPA receptor subunits. Neuropharmacology 38:635–644.
- 49. Lu W, Ziff EB (2005) PICK1 interacts with ABP/GRIP to regulate AMPA receptor trafficking. Neuron 47:407–421.
- 50. Rocca DL, Martin S, Jenkins EL, Hanley JG (2008) Inhibition of Arp2/3-mediated actin polymerization by PICK1 regulates neuronal morphology and AMPA receptor endocytosis. Nat. Cell Biol. 10:259–271.
- 51. Karlsen ML, Thorsen TS, Johner N, Ammendrup-Johnsen I, Erlendsson S, Tian X, Simonsen JB, Høiberg-Nielsen R, Christensen NM, Khelashvili G, et al. (2015) Structure of Dimeric and Tetrameric Complexes of the BAR Domain Protein PICK1 Determined by Small-Angle X-Ray Scattering. Structure [Internet] 23:1258–1270. Available from:
- http://www.cell.com/article/S0969212615001793/fulltext
- 52. Hanley JG (2008) PICK1: A multi-talented modulator of AMPA receptor trafficking. Pharmacol. Ther. 118:152–160.
- 53. Madsen KL, Thorsen TS, Rahbek-Clemmensen T, Eriksen J, Gether U (2012) Protein interacting with C kinase 1 (PICK1) reduces reinsertion rates of interaction partners sorted to Rab11-dependent slow recycling pathway. J. Biol. Chem.
- 54. Bjerggaard C, Fog JU, Hastrup H, Madsen K, Loland CJ, Javitch JA, Gether U (2004) Surface targeting of the dopamine transporter involves discrete epitopes in the distal C terminus but does not require canonical PDZ domain interactions. J. Neurosci.
- 55. Erlendsson S, Rathje M, Heidarsson PO, Poulsen FM, Madsen KL, Teilum K, Gether U (2014) Protein interacting with C-kinase 1 (PICK1) binding promiscuity relies on unconventional PSD-95/discs-large/ZO-1 homology (PDZ) binding modes for nonclass II PDZ ligands. J. Biol. Chem.
- 56. Pan L, Wu H, Shen C, Shi Y, Jin W, Xia J, Zhang M (2007) Clustering and synaptic targeting of PICK1 requires direct interaction between the PDZ domain and lipid membranes. EMBO J.
- 57. Jo S, Kim T, Iyer VG, Im W (2008) CHARMM-GUI: A web-based graphical user interface for CHARMM. J. Comput. Chem. 29:1859–1865.
- 58. Lee J, Cheng X, Swails JM, Yeom MS, Eastman PK, Lemkul JA, Wei S, Buckner J, Jeong JC, Qi Y, et al. (2016) CHARMM-GUI Input Generator for NAMD, GROMACS, AMBER, OpenMM, and CHARMM/OpenMM Simulations using the CHARMM36 Additive Force Field. J. Chem. Theory Comput. 12:405–413.
- 59. Huang J, Rauscher S, Nawrocki G, Ran T, Feig M, de Groot BL, Grubmüller H, MacKerell AD (2017) CHARMM36m: an improved force field for folded and intrinsically disordered proteins. Nat. Methods 14:71–73.
- 60. Berendsen HJC, van der Spoel D, van Drunen R (1995) GROMACS: A message-passing parallel molecular dynamics implementation. Comput. Phys. Commun. 91:43–56.
- 61. Pall S, Abraham MJ, Kutzner C, Hess B, Lindahl E Tackling exascale software challenges in

- molecular dynamics simulations with GROMACS. In: Lecture Notes in Computer Science (including subseries Lecture Notes in Artificial Intelligence and Lecture Notes in Bioinformatics). Vol. 8759.; 2015. pp. 3–27.
- 62. Abraham MJ, Murtola T, Schulz R, Páall S, Smith JC, Hess B, Lindah E (2015) Gromacs: High performance molecular simulations through multi-level parallelism from laptops to supercomputers. SoftwareX 1–2:19–25.
- 63. Hess B, Bekker H, Berendsen HJC, Fraaije JGEM (1997) LINCS: A linear constraint solver for molecular simulations. J. Comput. Chem. [Internet] 18:1463–1472. Available from: http://doi.wiley.com/10.1002/(SICI)1096-987X(199709)18:12%3C1463::AID-JCC4%3E3.0.CO;2-H
- 64. Nose S (1984) A unified formulation of the constant temperature molecular dynamics methods. J. Chem. Phys. [Internet] 81:511. Available from:
- http://link.aip.org/link/JCPSA6/v81/i1/p511/s1&Agg=doi%5Cnhttp://scitation.aip.org/content/aip/journal/jcp/81/1/10.1063/1.447334%5Cnhttp://jcp.aip.org/resource/1/jcpsa6/v81/i1/p511_s1%5Cnhttp://link.aip.org/link/?JCP/81/511/1
- 65. Hoover WG (1985) Canonical dynamics: Equilibrium phase-space distributions. Phys. Rev. A 31:1695–1697.
- 66. Larrimore KE, Kazan IC, Kannan L, Kendle RP, Jamal T, Barcus M, Bolia A, Brimijoin S, Zhan CG, Ozkan SB, et al. (2017) Plant-expressed cocaine hydrolase variants of butyrylcholinesterase exhibit altered allosteric effects of cholinesterase activity and increased inhibitor sensitivity. Sci. Reports 2017 71 7:1–14.
- 67. Atilgan C, Atilgan AR (2009) Perturbation-response scanning reveals ligand entry-exit mechanisms of ferric binding protein. PLoS Comput. Biol. 5.
- 68. Modi T, Banu Ozkan S (2018) Mutations utilize dynamic allostery to confer resistance in TEM-1 β -lactamase. Int. J. Mol. Sci. 19.
- 69. Campitelli P, Modi T, Kumar S, Banu Ozkan S The Role of Conformational Dynamics and Allostery in Modulating Protein Evolution. Annual Reviews Inc.; 2020 pp. 267–288.
- 70. Modi T, Risso V, ... SM-R-N, 2021 undefined Hinge-shift mechanism as a protein design principle for the evolution of β -lactamases from substrate promiscuity to specificity. nature.com. 71. McCammon JA, Harvey SC Dynamics of Proteins and Nucleic Acids. Cambridge University Press; 1987.
- 72. Newman MEJ, Girvan M (2004) Finding and evaluating community structure in networks. Phys. Rev. E Stat. Nonlinear, Soft Matter Phys. 69.
- 73. Grant BJ, Rodrigues APC, ElSawy KM, McCammon JA, Caves LSD (2006) Bio3d: an R package for the comparative analysis of protein structures. Bioinformatics [Internet] 22:2695–2696. Available from: http://www.ncbi.nlm.nih.gov/pubmed/16940322
- 74. Skjaerven L, Yao XQ, Scarabelli G, Grant BJ (2014) Integrating protein structural dynamics and evolutionary analysis with Bio3D. BMC Bioinformatics 15.
- 75. Grant BJ, Skjærven L, Yao XQ (2021) The Bio3D packages for structural bioinformatics. Protein Sci. 30:20–30.
- 76. Ferreiro DU, Hegler JA, Komives EA, Wolynes PG (2007) Localizing frustration in native proteins and protein assemblies. Proc. Natl. Acad. Sci. U. S. A. 104.
- 77. Parra RG, Schafer NP, Radusky LG, Tsai MY, Guzovsky AB, Wolynes PG, Ferreiro DU (2016) Protein Frustratometer 2: a tool to localize energetic frustration in protein molecules, now with electrostatics. Nucleic Acids Res. 44.
- 78. Rausch AO, Freiberger MI, Leonetti CO, Luna DM, Radusky LG, Wolynes PG, Ferreiro DU,

- Parra RG (2021) FrustratometeR: an R-package to compute local frustration in protein structures, point mutants and MD simulations. Bioinformatics 37.
- 79. Christensen NR, Čalyševa J, Fernandes EFA, Lüchow S, Clemmensen LS, Haugaard-Kedström LM, Strømgaard K (2019) PDZ Domains as Drug Targets. Adv. Ther.
- 80. Costescu BI, Gräter F (2013) Time-resolved force distribution analysis. BMC Biophys. 6:5.
- 81. Stevens AO, He Y (2022) Allosterism in the PDZ Family. Int. J. Mol. Sci. 23.
- 82. Kalescky R, Liu J, A PT-TJ of PC, 2015 undefined (2014) Identifying key residues for protein allostery through rigid residue scan. ACS Publ. 119:1689–1700.
- 83. McLaughlin Jr RN, Poelwijk FJ, Raman A, Gosal WS, Ranganathan R (2012) The spatial architecture of protein function and adaptation. Nat. 2012 4917422 491:138–142.
- 84. Lee HJ, Zheng JJ (2010) PDZ domains and their binding partners: Structure, specificity, and modification. Cell Commun. Signal.
- 85. Du Q-S, Wang C-H, Liao S-M, Huang R-B (2010) Correlation Analysis for Protein Evolutionary Family Based on Amino Acid Position Mutations and Application in PDZ Domain. PLoS One 5:e13207.
- 86. Stevens AO, Luo S, He Y (2022) Three Binding Conformations of BIO124 in the Pocket of the PICK1 PDZ Domain. Cells 2022, Vol. 11, Page 2451 11:2451.
- 87. Binder JL, Berendzen J, Stevens AO, He Y, Wang J, Dokholyan N V, Oprea TI (2022) AlphaFold illuminates half of the dark human proteins. Curr. Opin. Struct. Biol. [Internet] 74:102372. Available from:
- https://www.sciencedirect.com/science/article/pii/S0959440X22000513
- 88. Stevens AO, He Y (2022) Benchmarking the Accuracy of AlphaFold 2 in Loop Structure Prediction. Biomolecules [Internet] 12. Available from: https://www.mdpi.com/2218-273X/12/7/985
- 89. He Y, Liwo A, Weinstein H, Scheraga HA (2011) PDZ binding to the BAR domain of PICK1 is elucidated by coarse-grained molecular dynamics. J. Mol. Biol. [Internet] 405:298–314.